Archives of Biochemistry and Biophysics 600 (2016) 12–22

Contents lists available at ScienceDirect

Archives of Biochemistry and Biophysics

journal homepage: www.elsevier.com/locate/yabbi

Low sequence identity but high structural and functional conservation: The case of Hsp70/Hsp90 organizing protein (Hop/Sti1) of *Leishmania braziliensis*

Fernanda A.H. Batista [a, 1], Thiago V. Seraphim [a, 1], Clelton A. Santos [b], Marisvanda R. Gonzaga [a], Leandro R.S. Barbosa [c], Carlos H.I. Ramos [b, d], Júlio C. Borges [a, *]

[a] Instituto de Química de São Carlos, Universidade de São Paulo (USP), Av. Trabalhador Sãocarlense, 400 – CP 780, 13560–970, São Carlos, SP, Brazil
[b] Instituto de Química, Universidade Estadual de Campinas (UNICAMP), Rua José de Castro, s/n – Cidade Universitária – CP 6154, 13083-970, Campinas, SP, Brazil
[c] Instituto de Física, Universidade de São Paulo (USP), Av. Prof. Lineu Prestes, 748, CP 26077, São Paulo, SP, Brazil
[d] Instituto Nacional de Ciência e Tecnologia em Biologia Estrutural e Bioimagem, Av. Brigadeiro Trompowsky, s/n – Cidade Universitária, Ilha do Fundão, Rio de Janeiro, RJ, Brazil

ARTICLE INFO

Article history:
Received 22 February 2016
Received in revised form
16 April 2016
Accepted 16 April 2016
Available online 19 April 2016

Keywords:
Hop
Hsp90
TPR
Molecular chaperones
L. braziliensis
Protozoa

ABSTRACT

Parasites belonging to the genus *Leishmania* are subjected to extensive environmental changes during their life cycle; molecular chaperones/co-chaperones act as protagonists in this scenario to maintain cellular homeostasis. Hop/Sti1 is a co-chaperone that connects the Hsp90 and Hsp70 systems, modulating their ATPase activities and affecting the fate of client proteins because it facilitates their transfer from the Hsp70 to the Hsp90 chaperone. Hop/Sti1 is one of the most prevalent co-chaperones, highlighting its importance despite the relatively low sequence identity among orthologue proteins. This multi-domain protein comprises three tetratricopeptides domains (TPR1, TPR2A and TPR2B) and two Asp/Pro-rich domains. Given the importance of Hop/Sti1 for the chaperone system and for *Leishmania* protozoa viability, the *Leishmania braziliensis* Hop (LbHop) and a truncated mutant (LbHop^{TPR2AB}) were characterized. Structurally, both proteins are α-helix-rich and highly elongated monomeric proteins. Functionally, they inhibited the ATPase activity of *Leishmania braziliensis* Hsp90 (LbHsp90) to a similar extent, and the thermodynamic parameters of their interactions with LbHsp90 were similar, indicating that TPR2A-TPR2B forms the functional center for the LbHop interaction with LbHsp90. These results highlight the structural and functional similarity of Hop/Sti1 proteins, despite their low sequence conservation compared to the Hsp70 and Hsp90 systems, which are phylogenetic highly conserved.

1. Introduction

The heat shock response involves an increase in the levels of several proteins, known as molecular chaperones and/or as heat shock proteins (Hsps), a class of conserved proteins that play critical roles in protein folding, trafficking, activity and degradation [1,2]. An efficient and regulated cell stress response is mandatory for maintaining protein homeostasis and the viability of organisms, particularly for organism subjected to environmental changes [2]. Parasites belonging to the genus *Leishmania*, which are causative agents of three forms of leishmaniasis in mammalian hosts [3], are subject to extensive environmental changes during their life cycle. These parasites adopt an extracellular infective promastigote form, which develops in the alimentary tract of the sandfly vector and is

Abbreviations: AUC, Analytical ultracentrifugation; CD, circular dichroism; f/f_0, frictional ratio; MM, molecular mass; R_s, Stokes radius; R_0, Stokes Radius for a smooth and spherical particle; R_g, Radius of gyration; $s_{20,w}$, sedimentation coefficient at standard conditions; $s^0_{20,w}$, standard sedimentation coefficient at 0 mg mL^{-1} of protein; [θ], residual molar ellipticity; <λ>, center of spectral mass; SAXS, small angle X-ray scattering; aSEC, analytical size exclusion chromatography; p(r), particle distance distribution plot; ITC, isothermal titration calorimetry; ΔH_{app}, apparent enthalpy change; ΔS_{app}, apparent entropy change.

* Corresponding author. Instituto de Química de São Carlos, Universidade de São Paulo, USP, P.O. Box 780, Zip Code 13560-970, São Carlos, SP, Brazil.
E-mail address: borgesjc@iqsc.usp.br (J.C. Borges).

[1] These authors contributed equally for this work.

http://dx.doi.org/10.1016/j.abb.2016.04.008
0003-9861/

inoculated into a mammalian host during a blood meal; they can also have an intracellular amastigote form that differentiates and multiplies inside the macrophage phagolysosome, spreading the infection and causing the disease symptoms [1,2]. During this transition, changes in temperature and pH trigger this differentiation [3–5]; although the exact molecular mechanisms remain to be elucidated, it is already known that chaperones act as protagonists during this process [5–8]. In this scenario, the differentiation signals are linked to environmental stress, emphasizing the importance of molecular chaperones and Hsp for *Leishmania* biology [9].

The 82–96 kDa (Hsp90) and the 70 kDa (Hsp70) heat shock proteins are the main molecular chaperones found in the eukaryotic proteome [10–12]. The stress response in *Leishmania* is regulated by post-transcriptional mechanisms, such as alterations in mRNA stability. The Hsp genes are transcribed constitutively, and the transcription is not induced by heat shock [1,7]. Thus, the Hsp90/Hsp70 proteins account for approximately 4–5% of the total soluble protein level, even in non-stressed *Leishmania* promastigotes [2].

Hsp90 is an ATPase that interacts with partially folded, unfolded or misfolded proteins, assisting their correct folding/maturation or targeting them for degradation [11]. Hsp90 is a homodimer and contains three functional domains: an N-terminal domain (N-domain) containing the nucleotide-binding site; the middle domain (M-domain) involved in several functions, such as ATP hydrolysis and client protein and co-chaperone binding; and a C-terminal domain (C-domain) required for Hsp90 dimerization and interaction with co-chaperones [10,11]. The Hsp90 ATPase cycle includes passage through an open and a closed state, and these conformational changes are important for client protein stabilization [11,13]. Indeed, the co-chaperones appear to be the key elements that modulate the ATPase activity of these chaperones [9,14,15].

Co-chaperones are proteins that regulate the function of chaperones through direct interaction with them. For many co-chaperones, these interactions occur through their tetratricopeptide (TPR) domains, comprised of tandem repeats of a 34 amino acid motif that folds into antiparallel α-helices and is able to interact with the EEVD sequence belonging to the C-terminal tails of the cytoplasmic Hsp70/Hsp90 chaperones [16,17]. The yeast *stress-inducible protein 1* (Sti1), also known as *Hsp70/Hsp90 organizing protein* (Hop), is an important co-chaperone that can modulate the ATPase activity of both Hsp90 and Hsp70 through its TPR domains [18]. Hop/Sti1 inhibits the Hsp90 ATPase activity [19,20] and stimulates the ATPase activity of Hsp70 proteins [21].

Beyond the functions intrinsically related to the chaperone system, other Hop/Sti1 roles have been identified. It was reported that the human Hop/Sti1 (hHop) secreted by astrocytes binds to prion protein and is involved in the synthesis of this protein [22]. This finding suggests that the prion protein-Hop/Sti1 interaction modulates the pool of cellular proteins needed for proper neuronal function [22]. The Hop/Sti1 from *Leishmania major* (LmSti1) is implicated as the main target for humoral and cell-mediated immune responses during experimental murine leishmaniasis [23]. Furthermore, sera from patients with cutaneous leishmaniasis *(Leishmania major*), visceral leishmaniasis or post-kala-azar leishmaniasis *(Leishmania donovani*) exhibited reactivity toward recombinant LmSti1 [23]. Based on these results, LmSti1 has been used as part of a polyprotein antigen in a potential vaccine against leishmaniasis [24].

Hop/Sti1 is a multi-domain and monomeric protein composed of nine TPR motifs divided into three TPR domains (each containing three TPR motifs): TPR1, TPR2A and TPR2B [16,25]. TPR1 binds electrostatically to the Hsp70 C-terminal heptapeptide containing the PTIEEVD motif through a dicarboxylate clamp, whereas the TPR2A domain binds to the Hsp90 C-terminal pentapeptide containing the MEEVD motif, also through a dicarboxylate clamp [16,26]. Hydrophobic and van der Waals forces govern the TPR1 and the TPR2A interactions with Hsp70 and Hsp90, respectively [16]. TPR2B is able to interact with both chaperone motifs with lower affinity than those of the other TPR domains, because TPR2B has a less selective Hsp70/Hsp90 peptide-binding site [27]. Such lower affinities occur in the absence of a hydrophobic pocket in TPR2B, which enables TPR2B to accommodate both the methionine from Hsp90 and the energetically unfavorable conformation that the Hsp70 adopts to interact with TPR2B [27]. Importantly, a study of the Sti1 TPR2A-TPR2B comprising three TPR motifs plus an extra helix at the C-terminus revealed the existence of a rigid linker between the two TPR domains [27]. This linker guides the TPR domains to adopt an *S*-shaped structure with their peptide-binding pockets pointing towards opposite directions; this structure allows the simultaneous binding of TPR2A to the Hsp90 C-terminal domain and of TPR2B to Hsp70 [27]. The importance of this rigid linker, wherein the residues responsible for stabilizing the structure are conserved in different Hop/Sti1 orthologues, is emphasized by studies that demonstrated reduced protein function in response to flexibility in the linker [27].

Classical Hop/Sti1 also presents two Asp/Pro-rich domains (DP). One is localized after the TPR1 domain, and the other, after the TPR2B domain. Sti1 DP1 and DP2 are composed of six and five α-helices, respectively, which are important for *in vivo* client protein activation; additionally, DP1 is not able to replace DP2 in activation assays [27]. Unlike the observations for the linker between the TPR2A and TPR2B domains, the linker between the DP1 and TPR2A domains is flexible [27]. Last but not least, the TPR2A-TPR2B domains appear to be sufficient for promoting the inhibition of Hsp90 ATPase activity compared with that for full-length Sti1 [27,28]. The presence of DP2 is essential for supporting client protein activation *in vivo* [27]. Taken together, those observations lead to the proposal that the TPR1-DP1 module participates in the delivery of the client protein to the TPR2A-TPR2B-DP2 module, which is considered the center of activity of the protein [27,29].

Given the importance of Hop/Sti1 proteins for the Hsp70/Hsp90 chaperone machineries, in this work, we investigated the sequence, structure and function of the full-length *Leishmania braziliensis* Hop (LbHop) and its TPR1-DP1 deletion mutant ($LbHop^{TPR2AB}$). The proteins were produced, purified and structurally characterized through biophysical tools. The thermodynamic parameters of the molecular binding events between *Leishmania braziliensis* Hsp90 (LbHsp90) and the full-length LbHop, as well as the deletion mutant $LbHop^{TPR2AB}$, were determined. Assays aimed at elucidating the functional role of LbHop in the LbHsp90 ATPase cycle were performed. Our study reinforces the observation that Hsp90 is a conserved system among different phylogenetic branches and that the relatively low sequence conservation of Hop/Sti1 orthologues does not seem to alter their structural and functional features [30,31]. Understanding these sequence differences should clarify the fine-tuning mechanisms of Hsp90 regulation in the *L. braziliensis* protozoa, which might help to distinguish it from the host system.

2. Material and methods

2.1. Sequence analysis

The architecture of several Hop/Sti1 proteins was analyzed using the SMART server (http://smart.embl-heidelberg.de/) [32]. Sequence alignment of LbHop (NCBI ID: XP_001562145) with human (NCBI ID: P31948) and yeast (NCBI ID: CAA99217) orthologues (hHop and Sti1, respectively) was performed using the program

MUSCLE (http://www.ebi.ac.uk/Tools/msa/muscle/). Pairwise sequence alignment between LbHop and orthologue Hop/Sti1 proteins was performed using the EMBOSS Needle tool (http://www.ebi.ac.uk/Tools/psa/emboss_needle/).

2.2. Cloning, expression and purification

The coding DNA for full-length LbHop (1–547) was amplified from *L. braziliensis* genomic DNA by PCR using specific oligonucleotides and cloned into the pET23a vector (Novagen). For LbHop^{TPR2AB}, corresponding to LbHop from amino acids 170 to 547, the coding DNA was amplified using the pET23a:LbHop vector as a template and cloned into the pET28a vector (Novagen). Recombinant LbHop and LbHop^{TPR2AB} were expressed in the *Escherichia coli* BL21 (DE3) strain at the mid-log phase ($A_{600nm} \approx 0.6$) at 30 °C by the addition of 0.4 mM IPTG. After 4 h, cells were harvested by centrifugation. LbHop-expressing cells were resuspended in 25 mM Tris-HCl (pH 8.0), 20 mM NaCl, and 2 mM EDTA, whereas LbHop^{TPR2AB}-expressing cells were resuspended in 25 mM sodium phosphate (pH 7.4), 500 mM NaCl, and 20 mM imidazole; both were performed in the presence of 30 μg/mL lysozyme (Sigma) and 5 units of DNase (Sigma) and followed by 30 min of incubation on ice. Cells were disrupted by sonication and centrifuged for 20 min at 20,000 × g, the remaining supernatant was used for protein purification. LbHop was purified by ion exchange chromatography, using Macro-Prep High-Q Media (Bio-Rad) equilibrated with 10 mM Tris-Cl (pH 8.0) buffer containing 20 mM NaCl and 2 mM EDTA. The elution was performed using a linear gradient of 10 mM Tris-HCl (pH 8.0) buffer containing 500 mM NaCl and 2 mM EDTA. The fractions containing LbHop were dialyzed against 10 mM sodium phosphate (pH 7.4) buffer and subjected to affinity chromatography in CHT Ceramic Hydroxyapatite Type II Medium (Bio-Rad). LbHop elution was performed using a linear gradient of 10–500 mM sodium phosphate (pH 7.4). Lastly, size exclusion chromatography was performed using a Superdex 200 16/60 pg column (GE Healthcare Life Sciences), which had been previously equilibrated with the 25 mM Tris-HCl buffer (pH 8.0) containing 100 mM NaCl, 1 mM EDTA and 1 mM β-mercaptoethanol. For LbHop^{TPR2AB} purification, the supernatant was subjected to Ni^{2+}-affinity chromatography using a HisTrap HP column (GE Healthcare Life Sciences) with 25 mM sodium phosphate buffer (pH 7.4) containing 500 mM NaCl and 20 mM imidazole. LbHop^{TPR2AB} was eluted with the same buffer containing 500 mM imidazole, and the fraction was loaded into a Superdex 200 16/60 pg column (GE Healthcare), which had been previously equilibrated with the 25 mM Tris-HCl buffer (pH 8.0) containing 100 mM NaCl, 1 mM EDTA and 1 mM β-mercaptoethanol. LbHsp90 purification was performed as previously described [33]. Protein concentrations were measured spectrophotometrically at 280 nm, and the Sednterp program (http://sednterp.unh.edu/) was used to estimate the physicochemical parameters of the proteins from their amino acid sequences.

2.3. Spectroscopy experiments

Circular dichroism (CD) experiments were performed in a J-815 spectropolarimeter (Jasco) coupled to a Peltier-type system for temperature control. The CD spectra were collected in a 0.2 mm path length quartz cell containing approximately 4 μM LbHop or LbHop^{TPR2AB} dissolved in the 25 mM Tris-HCl buffer (pH 8.0) containing 100 mM NaCl, 1 mM EDTA and 1 mM β-mercaptoethanol. Secondary structure estimation was performed using the DichroWeb server [34]. All CD data were normalized to the residual molar ellipticity ([θ]).

The intrinsic fluorescence emission measurements were performed in an F-4500 fluorescence spectrophotometer (Hitachi) at 20 °C. The fluorescence emission spectra of 5 μM LbHop or LbHop^{TPR2AB} in the buffer described above were measured in a 1 × 0.2 cm quartz cuvette after sample excitation at 280 nm. The fluorescence emission spectra were analyzed using the maximum emission wavelength (λ_{max}) and the center of spectral mass (<λ>), which was estimated as previously described [33].

2.4. Hydrodynamic experiments

Analytical size exclusion chromatography (aSEC) experiments were conducted as previously described [33]. Each protein at a 30 μM concentration was loaded in a Superdex 200 10/300 GL column (GE Healthcare) equilibrated with 25 mM Tris-HCl (pH 8.0) buffer containing 100 mM NaCl, 2 mM EDTA and 1 mM β-mercaptoethanol.

Sedimentation velocity analytical ultracentrifugation (SV-AUC) experiments were performed in an Optima XL-A analytical ultracentrifuge (Beckman) with the AN-60 Ti rotor at 35,000 rpm and 20 °C. Sedimentation of LbHop was monitored using the absorbance at 275 and 280 nm, whereas LbHop^{TPR2AB} was monitored using the absorbance at 230 and 280 nm, depending on the protein concentration. The experiments were performed for protein concentrations ranging from 100 to 1000 μg/mL dissolved in the buffer described above. AUC data were treated by the SedFit 12.2 software [35] using the frictional ratio (f/f_0) as a regularization parameter. The *s*-values were normalized to standard conditions ($s_{20,w}$ − sedimentation coefficient at 20 °C, in water). The buffer density (1.00369 g/mL) and viscosity (0.00102 Poise), as well as the partial specific volume of LbHop (0.7282 mL/g) and LbHop^{TPR2AB} (0.7287 mL/g), were estimated using the Sednterp program. The $s^0_{20,w}$-value ($s_{20,w}$ at 0 mg/mL protein) was estimated by linear regression analysis of the graph of the $s_{20,w}$-values as a function of protein concentration [36].

2.5. Small angle X-ray scattering

Small angle X-ray scattering (SAXS) experiments were performed at the Brazilian Synchrotron Light Laboratory (LNLS-CNPEM, Campinas, Brazil) at the SAXS1 and SAXS2 beamlines. LbHop data were collected at 0.8, 1.3 and 1.8 mg/mL, and LbHop^{TPR2AB} data were acquired at 1.4, 4.3 and 8.5 mg/mL, with both proteins in the 25 mM Tris-HCl buffer (pH 7.5) containing 100 mM NaCl, 1 mM EDTA and 1 mM β-mercaptoethanol. The scattering curves were treated, normalized by the concentration and checked for monodispersity and protein aggregation using Guinier analysis and the PRIMUS program [37]. The particle distance distribution functions (p(r)) were calculated by indirect Fourier transform using the GNOM program [38]. Fifteen *ab initio* models for each protein were generated by the DAMMIN program [39] and merged using the DAMAVER package [40]. The hydrodynamic parameters of the final models were calculated using the Hydropro program [41]. The three-dimensional structures of the hHop (TPR1 PDB: 1ELW) [16] and Sti1 (DP1 PDB: 2LLV; DP2 PDB: 2LLW; TPR2AB PDB: 3UQ3) [27] domains were superimposed on the *ab initio* models by the UCSF Chimera software [42]. The SAXS data and the *ab initio* models obtained for LbHop and LbHop^{TPR2AB} can be found in the Small Angle Scattering Biological Data Bank (http://www.sasbdb.org/) under the access codes SASDB54 and SASDB64, respectively.

2.6. Isothermal titration calorimetry

Isothermal titration calorimetry (ITC) experiments were performed at 20 °C using an iTC200 microcalorimeter (GE Healthcare Life Sciences). LbHsp90, LbHop and LbHop^{TPR2AB} were dialyzed

extensively against 40 mM HEPES buffer (pH 7.5) containing 100 mM KCl. Aliquots of 1.2–1.4 μL of LbHop or LbHop^{TPR2AB} at 160–280 μM were injected into 203.8 μL of LbHsp90 at approximately 11 μM (as dimers). The data were analyzed by Microcal Origin software using the One Set of Sites model to calculate the apparent enthalpy change (ΔH_{app}), stoichiometry (n), association constant (K_A), and apparent entropy change (ΔS_{app}), which was calculated from the ΔH_{app} and K_A experimental values using the equation $\Delta S = (RTlnK_A + \Delta H)/T$. The heat of the ligand dilution was determined from its titration into the buffer solution and by a correction procedure in which the end of curve for the titration with the protein receptor was subtracted from the data.

2.7. ATPase activity inhibition

The inhibition of LbHsp90 ATPase activity was evaluated using an EnzChek Phosphate Assay kit (Molecular Probes) as previously shown [43]. LbHsp90 (1 μM dimers) was incubated at 37 °C for 3 h with 3 mM ATP in the presence of increasing concentrations of LbHop and LbHop^{TPR2AB} (0–10 μM). The positive control was LbHsp90 with ATP only. All samples were prepared in 40 mM HEPES buffer (pH 7.5) containing 100 mM KCl. The P_i released (μM/min) was plotted as a function of the LbHop or LbHop^{TPR2AB} concentrations and represented as the relative ATPase activity. A negative control was obtained using BSA. The data were fitted with a dose-response function to obtain the 50% inhibitory concentration value (IC_{50}).

3. Results and discussion

3.1. LbHop shares common features with orthologue Hop/Sti1 proteins

Hop/Sti1 is a co-chaperone connecting the Hsp70 and Hsp90 chaperone systems through interaction with the EEVD motif located at the C-terminus of both molecular chaperones by the formation of a dicarboxylate clamp [16,27,44,45]. To determine the LbHop organization and its conservation in terms of the well-studied yeast and human counterparts, domain prediction and sequence alignment analyses were performed (Fig. 1). LbHop showed identities of 35% and 39% with Sti1 and hHop, respectively; in addition, Sti1 and hHop share 39% identity. Despite the relative low sequence identities, LbHop showed a domain organization similar to those of Sti1 and hHop; it contained three TPR domains and two DP domains. The LbHop TPR1 was found to be approximately 45% identical to those of the yeast and human proteins. TPR2A and TPR2B displayed a conservation of 31% and 43%, respectively, with respect to the yeast orthologue, and 46% and 48%, respectively, in relation to the human counterpart. The DP1 domain showed an identity of around 20% with the corresponding Sti1 and hHop sequences, whereas the DP2 domain showed 50% identity with these Hop/Sti1 orthologues. Twelve Hop/Sti1 proteins other than Sti1 and hHop were analyzed to determine their identity with LbHop and their domain organization (Table 1). Despite their identity with LbHop, all Hop/Sti1 proteins analyzed in this study contained three TPR domains, except the *Entamoeba histolytica* protein. The presence of DP1 or DP2 domains might not be a rule of thumb, and the lengths of linker regions between the TPR1 and TPR2A domains were variable. However, how such differences could influence the Hop/Sti1 function has to be further investigated.

Comparing LbHop and the well-studied Sti1 and hHop, the amino acid residues involved in the dicarboxylate clamp formation with the EEVD motif of Hsp70/Hsp90 are conserved inside the TPR1 and TPR2A domains (Fig. 1, black filled bars). In general, these findings suggest that LbHop could interact with LbHsp70/LbHsp90 through well-established interactions. Interestingly, although important residues for the specificity of the Hsp90 interaction were conserved in all three analyzed proteins, the residues that are important for Hsp70 recognition showed some variability (Fig. 1, black empty bars). Comparing the TPR2B domain among the three sequences, the amino acid residues involved in the dicarboxylate clamp formation were less conserved than those in the TPR1 and TPR2A domains (Fig. 1, black filled bars), mainly for Sti1, as previously observed [27]. However, the TPR2B domains of all three proteins have features suggesting they are able to interact with the Hsp70/Hsp90 EEVD motif.

3.2. LbHop and LbHop^{TPR2AB} were obtained soluble and folded

To study the LbHop structure and its effect on LbHsp90, we produced the full-length protein (Fig. 2A, *top*) and the LbHop^{TPR2AB} construct (Fig. 2B, *top*). LbHop and LbHop^{TPR2AB} were produced, as described in the Material and methods section, and were purified from the soluble fraction until homogeneity, as indicated by the bands observed using SDS-PAGE (Fig. 2A, *bottom*, *lane 5*; Fig. 2B, *bottom*, *lane 4*). For the bands correspond to each of the two proteins, the run profile was consistent with the predicted values of molecular mass (MM) for LbHop (62.5 kDa) and LbHop^{TPR2AB} (45.6 kDa).

Because LbHop and LbHop^{TPR2AB} were soluble and purified until homogeneity, we verified the structure of both proteins. Circular dichroism spectra of both proteins (Fig. 3A) showed characteristic α-helix profiles. Spectral deconvolution indicated α-helix contents of approximately 75% and 69% for LbHop and LbHop^{TPR2AB}, respectively, whereas the β-sheet content was of about 5% for both proteins. These results are in agreement with those expected for TPR-containing proteins, which typically fold into three repetitions of the helix-turn-helix motifs known as TPR motifs [16,46]. Indeed, these findings are in full agreement with the secondary structure observed for the human and *Drosophila* Hop/Sti1 (37% of identity with LbHop) counterparts [47,48]. The local tertiary structure was evaluated using the intrinsic tryptophan fluorescence (Fig. 3B). The results showed that LbHop and LbHop^{TPR2AB} possess local tertiary structure and that the tryptophan residues are located in a partially solvent-exposed region. In fact, each LbHop TPR domain contains one tryptophan residue, and the deletion of the TPR1 domain did not cause a shift in the fluorescence spectra. Altogether, our results showed that the obtained LbHop and LbHop^{TPR2AB} were pure and folded, with a predominantly α-helical secondary structure.

3.3. LbHop and LbHop^{TPR2AB} are elongated monomers in solution

The *in vitro* oligomeric state of Hop was consistently investigated. Previous studies found hHop as dimers [49], however hHop, Sti1 and dHop were also found as monomers [28,47] or in a monomer-dimer equilibrium [28,48]. To investigate the oligomeric state of LbHop and LbHop^{TPR2AB}, we performed aSEC experiments (Fig. 3C and Table 2). First, both profiles are consistent with homogeneous solutions. Second, LbHop eluted between a MM of 160 and 67 kDa, which could indicate that this protein is dimeric; in contrast, LbHop^{TPR2AB} eluted between a MM of 45 kDa and 29 kDa, in accordance with a monomeric model.

To determine the LbHop oligomeric state, SV-AUC experiments were carried out (Fig. 3D and Table 2) because its hydrodynamic properties could be attributed to either an elongated monomer or a globular dimer. Both LbHop and LbHop^{TPR2AB} sedimented as only one species with MMs of 63 ± 2 kDa and 42 ± 1 kDa, respectively. In addition, the f/f_0-values obtained for LbHop (1.65 ± 0.04) and LbHop^{TPR2AB} (1.52 ± 0.06) indicated that they were elongated

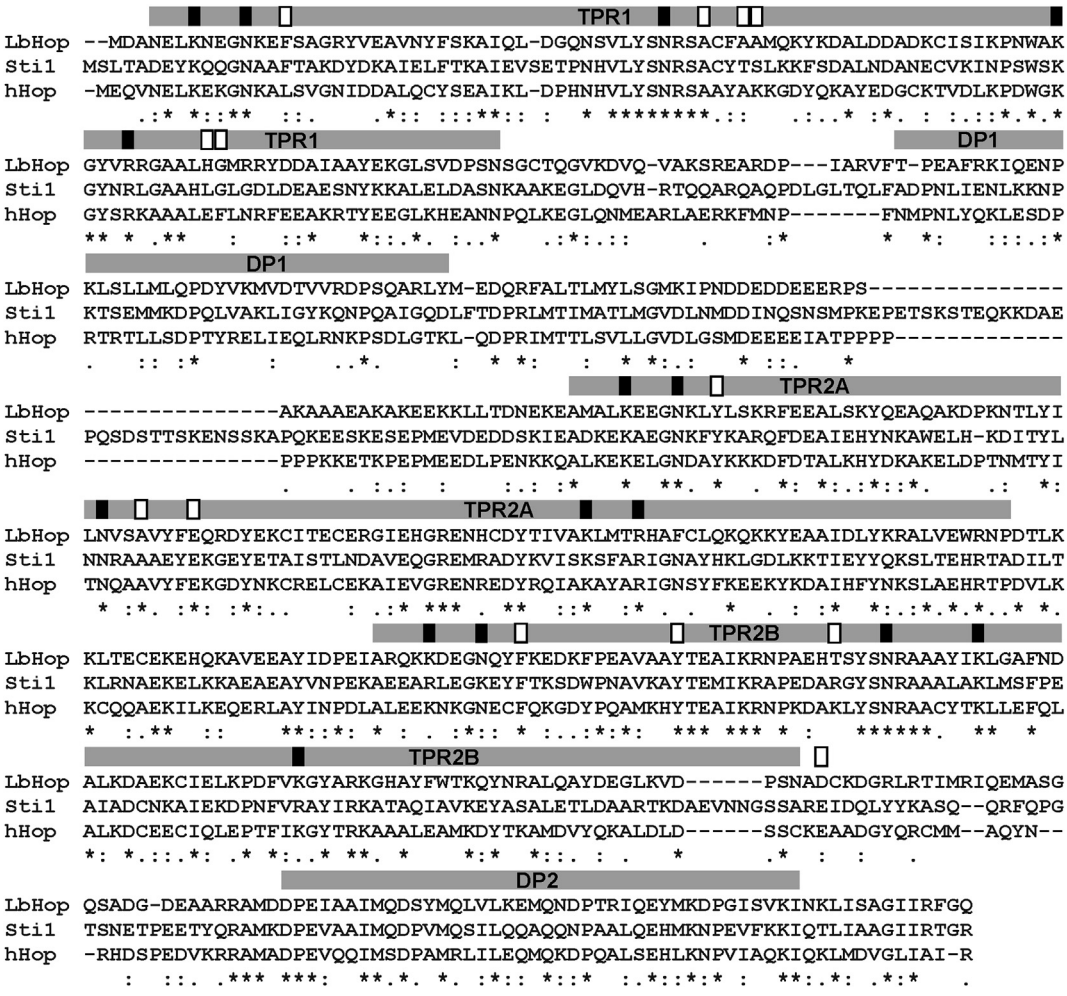

Fig. 1. Sequence analysis of LbHop. LbHop was aligned with the yeast and human counterparts, Sti1 and hHop. The LbHop domain organization is shown with gray bars, and the residues directly involved in dicarboxylate clamp-mediated Hsp70/Hsp90 interaction are indicated by black filled bars. Black empty bars indicate the residues involved in the Hsp70/Hsp90 interaction based on previous Sti1 work [16,27]. Stars, colons and dots are identical, strongly similar and weakly similar residues, respectively.

particles. In spite of previous evaluations, which pointed that Hop protein should behaves as dimers, Yi et al. demonstrate indubitably, that the Hop protein is a monomer in solution [47]. In this way, hydrodynamic properties of LbHop were in agreement with the monomeric species of hHop [47,48] confirming that LbHop and LbHop^{TPR2AB} behave as elongated monomers in solution.

3.4. LbHop has an elongated shape common to other Hop/Sti1 proteins.

To investigate the overall structure and dynamics and thus further elucidate the mechanistic aspects of Hop/Sti1 function, SAXS experiments were performed over the past years using yeast and human counterparts [19,49,50]. To determine the low-resolution structure of the LbHop protein, we performed SAXS experiments with the full-length and TPR2AB constructs (Fig. 4). The LbHop and LbHop^{TPR2AB} SAXS curves are depicted in Fig. 4A. Both proteins were found as monodisperse and monomeric systems, as verified by Guinier analysis and MM estimation (Fig. 4A, *inset;* Table 2). Fig. 4B shows the p(r) and revealed that LbHop and LbHop^{TPR2AB} have D_{max} values of around 180 Å and 140 Å, respectively. Such dimensions are in close agreement with those determined for hHop [19,49] and are of the same order as that determined for LbHsp90 (unpublished results). Interestingly, Sti1 possess a longer linker region between the DP1 and TPR2A domains, whereas hHop and LbHop do not (see Fig. 1). Such features could be responsible to the higher D_{max} value observed for Sti1 [19,50]. In addition to such observations, the LbHop^{TPR2AB} construct displayed a similar size as that of the TPR2A-TPR2B-DP2 construct of Sti1 [50], reinforcing the idea that the linker region between the DP1 and TPR2A domains is the reason for the higher D_{max} value observed for Sti1. In addition, the agreement between the LbHop Rg values estimated by the Guinier analysis and from the p(r) curve (Table 2) attests to the quality of the SAXS data. Moreover, Kratky analysis (Fig. 4B, *inset*) clearly showed that LbHop and LbHop^{TPR2AB} were well-folded during the SAXS experiments.

In 2008, Onuoha et al. [49] proposed a model where hHop behaves as dimers in a quaternary structure described as a butterfly-like model. However, the validity of this model is controversial, especially because the monomeric nature of human and yeast Hop/Sti1 was demonstrated in later SAXS studies [19,47,50]. Therefore, we constructed *ab initio* models for LbHop monomeric constructs using dummy atoms in a simulated-annealing procedure. The LbHop *ab initio* model (Fig. 4C) easily accommodated the three-dimensional TPR1 [16], DP1, TPR2A, TPR2B and DP2 [27] structures and showed an elongated shape resembling the monomeric form of the Sti1 model [49]. The hydrodynamic properties of the full-length protein model were similar to the experimentally

Table 1
Identity and domain organization of LbHop and orthologue proteins.

Organism	NCBI ID	Identity[#] (%)	Domain organization[&]
Leishmania braziliensis	XP_001562145	100	
Leishmania major	CAJ02290	93	
Trypanosoma cruzi	AAC97378	52	
Arabdopsis thaliana	Q9LNB6	40	
Homo sapiens	P31948	39	
Mus musculus	Q60864	39	
Sus scrofa	XP_003353842	39	
Rattus norvegicus	NP_620266	39	
Bos taurus	NP_001030569	39	
Drosophila melanogaster	NP_477354	37	
Plasmodium falciparum	AAN36937	37	
Schizosaccharomyces pombe	CAB39910	36	
Saccharomyces cerevisiae	CAA99217	35	
Candida albicans	AAZ41381	33	
Entamoeba histolytica	XP_650088	17	

[#]The identity values are respective to the LbHop.
[&]TPR: TPR motifs, STI1: DP1 or DP2 motifs; pink rectangle: low complexity region; green rectangle: coiled-coil.

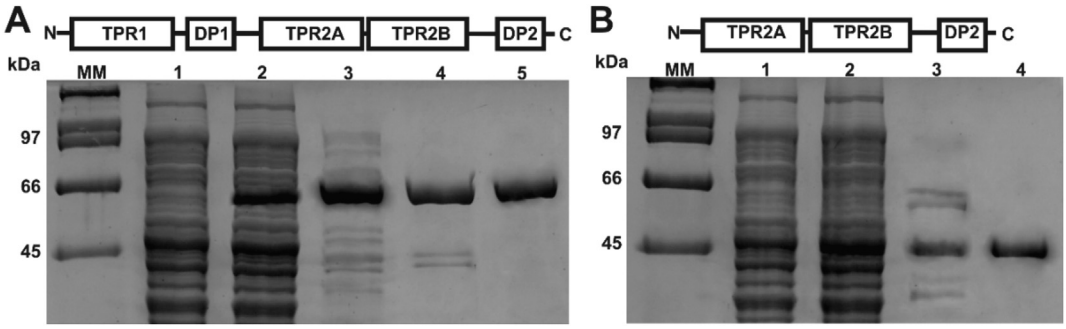

Fig. 2. LbHop and LbHop^{TPR2AB} production and purification. A) and **B)**, *top*: scheme of the LbHop and LbHop^{TPR2AB} constructs. **A)** and **B)**, *bottom*: SDS-PAGE for evaluating the purification process of LbHop and LbHop^{TPR2AB}, respectively, indicating both proteins were obtained with high purity (>95%). MM: molecular mass markers; lane 1 of both gels: cell lysate before induction; lane 2: cell lysate after induction; lane 3 (Fig. A): protein eluted from ion exchange chromatography; lane 3 (Fig. B): protein eluted from affinity chromatography; lane 4 (Fig. A) proteins eluted from ceramic hydroxyapatite chromatography; lane 5 (Fig. A) and 4 (Fig. B): proteins eluted from SEC.

determined values, except the D_{max} value (Table 2). This discrepancy may be due to the flexibility between the DP1 and TPR2A domains because the Hydropro program does not take into account this flexibility when it is determining the hydrodynamic properties of a rigid *ab initio* model. The LbHop^{TPR2AB} *ab initio* model (Fig. 4D) also displayed an elongated shape in solution; this shape fit very well with the three-dimensional structures of the TPR2A, TPR2B and DP2 domains [27]. In contrast to the findings for the full-length protein, the hydrodynamic properties estimated using the LbHop^{TPR2AB} low-resolution model were very similar to the experimental ones (Table 2). This difference may be due to both the lack of flexibility, such as the linker between the DP1 and TPR2A domains, and the presence of a rigid linker between TPR2A and TPR2B. These data clearly reveal the extended shape and modular behavior of LbHop, which is compatible with a mechanism that allows interactions with both the Hsp90 and Hsp70 molecular chaperones.

3.5. *LbHop and LbHop^{TPR2AB} interact with LbHsp90 and inhibit its ATPase activity.*

The interaction between both LbHop constructs and LbHsp90 was studied using ITC (Fig. 5). The interactions were exothermic and followed a stoichiometry of 1 molecule of LbHop or LbHop^{TPR2AB} per dimer of LbHsp90. The measured K_D values of the interaction of LbHop and LbHop^{TPR2AB} with LbHsp90 were 1.0 ± 0.2 μM (Fig. 5A) and 0.9 ± 0.1 μM (Fig. 5B), respectively. The contribution of the ΔH_{app} and ΔS_{app} to the LbHop-LbHsp90 interaction were −15.6 ± 0.3 kcal/mol and −25.8 ± 0.9 cal/mol/deg, respectively. For the LbHop^{TPR2AB}-LbHsp90 interaction, the measured

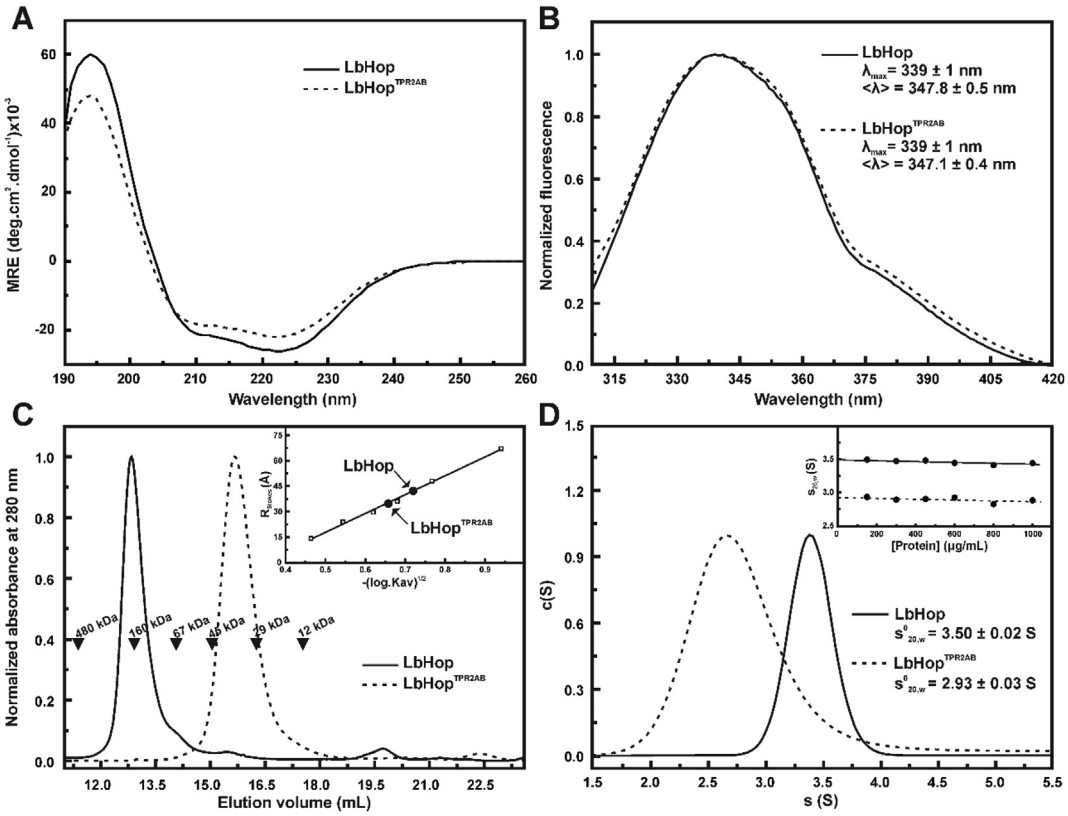

Fig. 3. Structural characterization of LbHop and LbHop^{TPR2AB}. A) Circular dichroism spectra of LbHop and LbHop^{TPR2AB} showing a characteristic α-helix profile. **B)** Tryptophan fluorescence spectra showing that LbHop and LbHop^{TPR2AB} possess local tertiary structure. **C)** aSEC profiles of LbHop and LbHop^{TPR2AB} indicating that both proteins eluted as single peaks. *Inset*: Determination of the Stokes radius. Standard proteins are shown as empty circles. **D)** Sedimentation velocity experiments displaying the sedimentation of LbHop and LbHop^{TPR2AB} as single species. *Inset*: Determination of $s^0_{20,w}$ by linear regression analysis.

Table 2
Spectroscopic and hydrodynamic features of LbHop and LbHop^{TPR2AB} proteins.

Techniques	Properties	Proteins	
		LbHop	LbHop^{TPR2AB}
Theoretical[a]	MM (kDa)	62.5	45.6
	R_0 (Å)	26	24
aSEC	R_S (Å)	42 ± 1	35 ± 1
	f/f_0	1.65 ± 0.05	1.45 ± 0.05
SV-AUC	$s^0_{20,w}$ (S)	3.50 ± 0.02	2.93 ± 0.03
	MM (kDa)	63 ± 2	42 ± 1
	f/f_0	1.65 ± 0.04	1.52 ± 0.06
SAXS	$Rg_{Guinier}$ (Å)	45 ± 1	38 ± 2
	$Rg_{p(r)}$ (Å)	46.8 ± 0.2	40.8 ± 0.2
	MM (kDa)	63 ± 5	44 ± 4
	D_{max} (Å)	180 ± 10	140 ± 10
Hydropro[b]	R_S (Å)	40	37
	Rg (Å)	40	38
	D_{max} (Å)	148	138
	$s_{20,w}$ (S)	3.6	2.8

[a] Obtained from amino acid composition by the Sednterp program.
[b] Values calculated for the *ab initio* models generated from SAXS data.

ΔH_{app} and ΔS_{app} were -17.9 ± 0.2 kcal/mol and -33.4 ± 0.6 cal/mol/deg, respectively (Table 3). The nearly equal affinity displayed by both constructs indicated that the domains in LbHop^{TPR2AB} are sufficient to promote the proper interaction with LbHsp90, as expected from the results reported for other Hop/Sti1 proteins [27].

The observed thermodynamic signature indicated that the LbHop-LbHsp90 interaction is driven by a large favorable enthalpy, and it is accompanied by a large entropy penalty, which may be due to a conformational change in one or both proteins due to the binding event [28,51]. Such unfavorable entropy can be, at least partially, explained by the interaction mode between the two proteins. A similar unfavorable entropy was previously reported for the LbHsp90 interaction with other co-chaperones that restricts Hsp90 to less flexible conformations [43,52]. Beyond the canonical interaction of the Hsp90 C-terminal peptide with the Hop/Sti1 TPR2A, it was also found that the Hsp90 M-domain is able to interact with TPR2B [27,49,53]. The importance of this additional interaction can be observed in ITC studies where the interaction between the full-length human Hsp90 and hHop proteins displayed a K_D of 0.69 ± 0.04 μM in contrast to a K_D of 4.3 ± 0.2 μM for the human Hsp90 C-domain and full-length Hop/Sti1 proteins, indicating the importance of additional contacts (beyond the C-domain) for the Hsp90-Hop/Sti1 interaction [49]. In this context, the TPR2B domain is positioned between the two Hsp90 subunits, sterically precluding the rearrangement of the Hsp90 M-domain during the ATPase cycle [27] and adding an entropic penalty to the interaction. Indeed, the stable *S*-shaped conformation found for the TPR2A and TPR2B domains is known to be physiologically necessary because a mutation that increases the flexibility of the linker between these domains leads to a reduction in the Sti1-dependent glucocorticoid receptor activity [27].

The observed thermodynamic behavior for the LbHop:LbHsp90 interaction seems to be a hallmark of the Hop/Sti1-Hsp90 interaction because it was also observed for the corresponding yeast and human systems [28,49]. The affinity constants found in these three cases are of the same order and, together with the enthalpic and entropic contributions (Table 3), they reflect the conservation of the

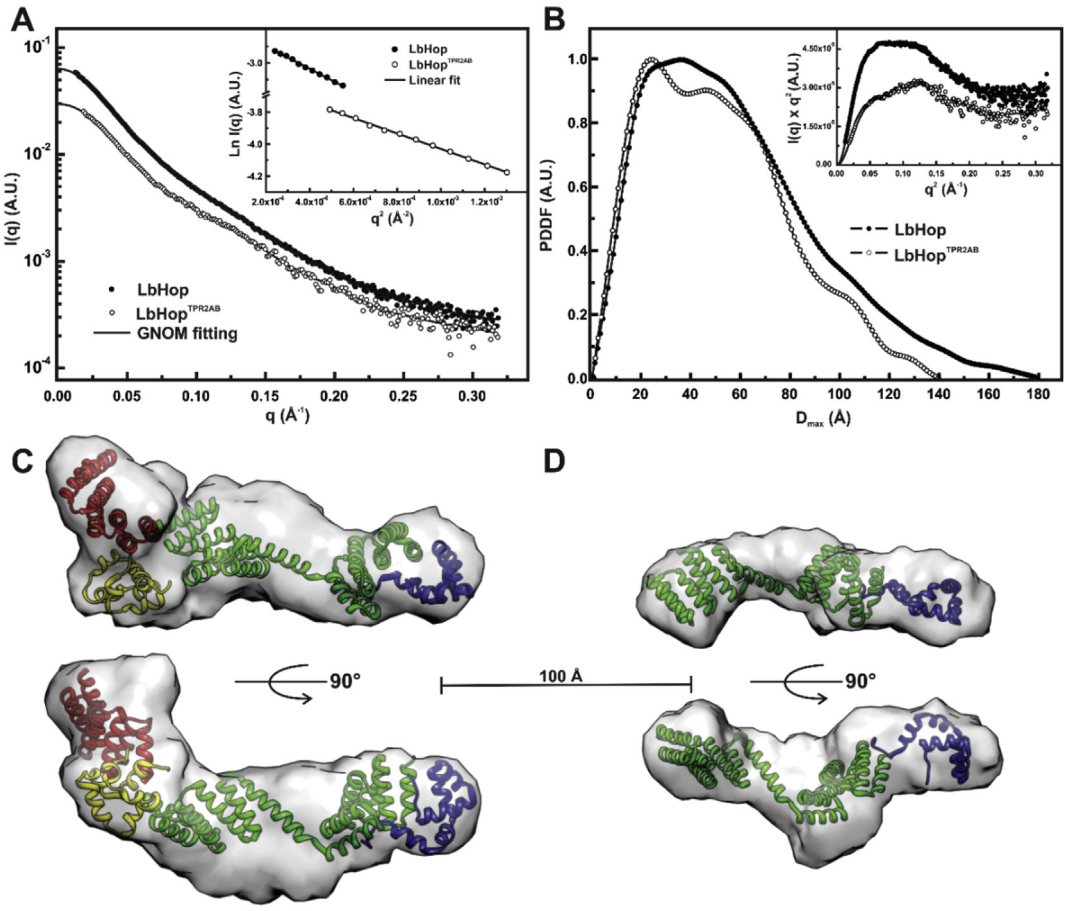

Fig. 4. Low-resolution structure of LbHop and LbHop^{TPR2AB}. A) SAXS curves for the full-length LbHop and the LbHop^{TPR2AB} constructs. *Inset*: Guinier analysis of the SAXS curves showing monodisperse systems. **B)** Particle distance distribution function of the LbHop constructs emphasizing their elongated shapes. *Inset*: Kratky plot indicating that the proteins were folded during the SAXS experiments. *Ab initio* models of the **C)** LbHop and **D)** the LbHop^{TPR2AB} constructs. The three-dimensional structures available for the domains of Sti1 were superimposed manually on the low-resolution structures.

interaction mode between Hsp90 and the Hop/Sti1 co-chaperone.

Despite the agreement observed among our data and those from other organisms, the stoichiometry was surprisingly divergent. We observed that one molecule of LbHop or LbHop^{TPR2AB} binds per LbHsp90 dimer, whereas two Sti1 and hHop molecules interact with yeast and human Hsp90 [28,49]. Despite the observed dimer form of hHop [28,49], an extensive study of hHop [47,48] demonstrated that the Hop/Sti1 protein is an elongated monomer is solution (which can explain the discrepancies with the previous results). The formation of disulfide-linked dimers in the absence of fresh reducing agents was also reported [47]. In agreement with these data, we identified that LbHop and LbHop^{TPR2AB} behaved as monomers in solution in the tested conditions using SAXS and AUC studies. Our ITC results were obtained in the absence of reducing agents, similarly to the yeast experiments; however, our experiments differed because our proteins were maintained in a reductive buffer until the dialysis step intended for the ITC experiments, thus likely avoiding the formation of disulfide-linked dimers. The possible presence of disulfide-linked Sti1 dimers should explain the discrepancy between the stoichiometry found for Sti1 and LbHop because the authors reported that the Sti1 behaves like a dimer [28].

3.6. Hsp90 ATPase activity inhibition

Hop/Sti1 is an Hsp90 ATPase activity inhibitor because its interaction promotes the stabilization of the open, client protein-loading conformation of Hsp90 [20,54]. The same inhibition behavior was verified for hHop, as well as for the TPR2A–TPR2B construct of both Sti1 and hHop [19,27]. The effect of LbHop and LbHop^{TPR2AB} on the LbHsp90 ATPase activity was similar to those observed for the yeast and human orthologues. As indicated in Fig. 6A, the phosphate released by LbHsp90 in the presence of LbHop or LbHop^{TPR2AB} was reduced to approximately 10% of the amount observed in the absence of the co-chaperone. Moreover, the IC_{50} values found for both constructs were of about 2 μM. This effect indicated that LbHop-LbHsp90 interaction is specific because the phosphate release was not affected by the presence of BSA, a protein that cannot interact with LbHsp90 (Fig. 6B).

In the same way, Sti1 also exhibits a marked inhibitory effect on the ATPase activity of Hsp90, with an IC_{50} of approximately 2 μM [28]. The inhibitory activity was also verified for the LbHop^{TPR2AB} protein in which the Hsp70 specific interaction site is missing. Similarly, a Sti1 construct lacking TPR1 was sufficient to promote the inhibition of the Hsp90 ATPase activity [27,28]. According to Schmid et al. [27], neither the TPR2A or TPR2B domains alone or together were able to produce an inhibitory effect; however, the Sti1 protein and its truncated TPR2A-TPR2B-DP2 and TPR2A–TPR2B constructs were equally effective at promoting the ATPase inhibition [27]. One possible explanation for this finding is that the two domains remain together due to the presence of a rigid linker region, which orientates them in a *S*-shaped conformation

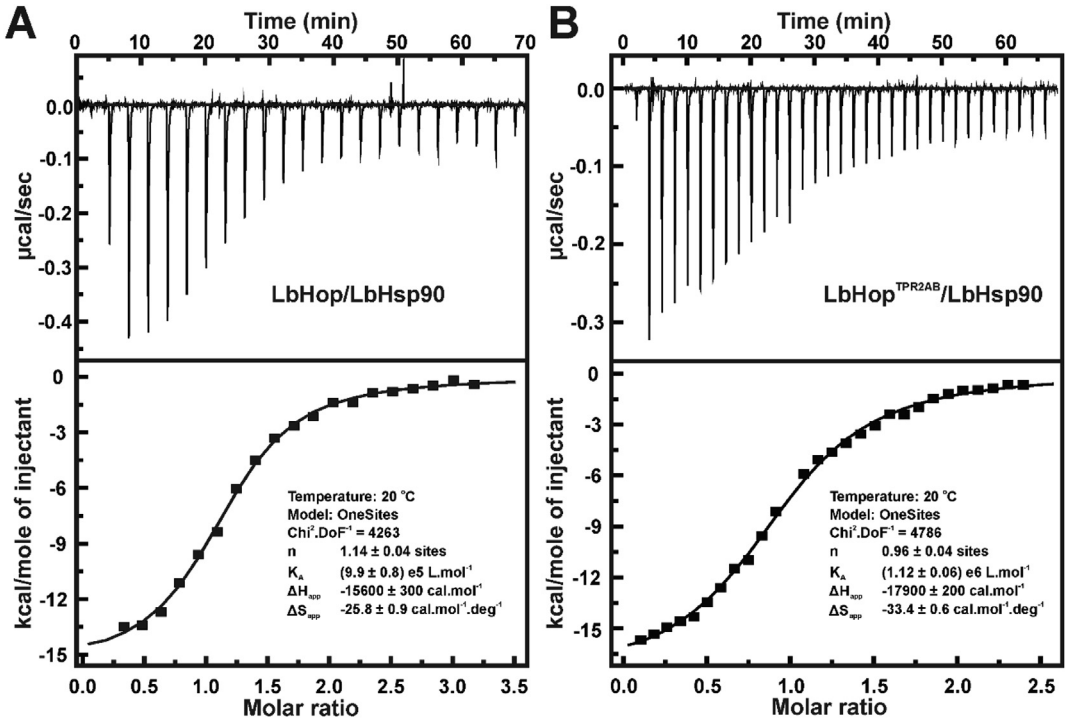

Fig. 5. Interaction of LbHsp90 with either LbHop or LbHop^{TPR2AB} verified by ITC. A) 230 µM LbHop and B) 106 µM LbHop^{TPR2AB} were titrated in 11 µM LbHsp90 at 20 °C. The thermodynamic parameters of both interactions were derived from the nonlinear least-squares fitting implemented by the Origin software.

Table 3
Thermodynamic data of Hop/Sti1:Hsp90 interactions obtained by ITC at similar conditions.

Interacting partners	Thermodynamic parameters				Reference
	ΔH_{app} (kcal mol^{-1})	ΔS_{app} (cal mol^{-1} K^{-1})	K_D (µM)	n	
LbHop: LbHsp90	−15.6 ± 0.3	−25.8	1.0 ± 0.2	1.14 ± 0.04[a]	Here
LbHop^{TPR2AB}: LbHsp90	−17.9 ± 0.3	−33.4	0.9 ± 0.1	0.96 ± 0.04[a]	Here
Sti1: yHsp90	−27.9 ± 0.1	−64	0.33 ± 0.03	–	[28]
hHop: hHsp90	−13.2 ± 0.1	−16.3	0.69 ± 0.04	–	[49]

[a] Considering Hsp90 as dimers.

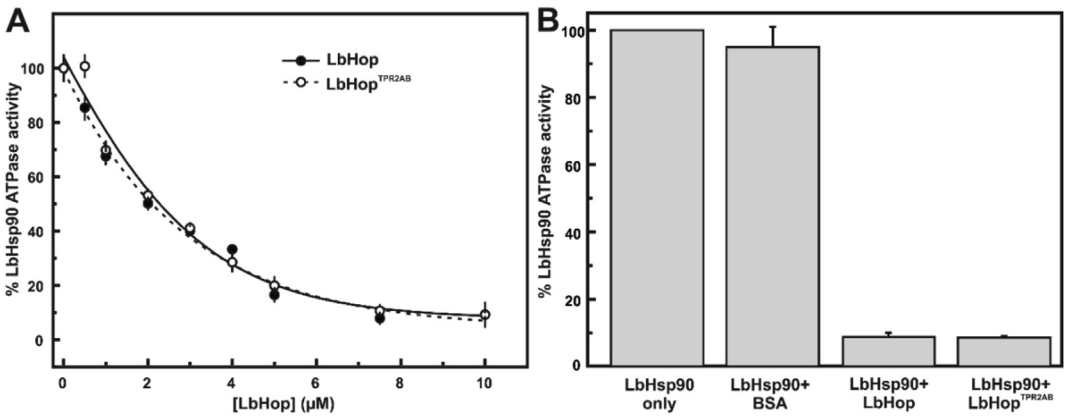

Fig. 6. Hsp90 ATPase activity inhibition assay. A) LbHsp90 was incubated with increasing concentrations of LbHop or LbHop^{TPR2AB}, followed by the addition of ATP; then, the Pi released was examined. The obtained data were fit a dose-response curve using Origin 8.1 software, and the IC_{50} values were determined. B) The ATPase activity of Hsp90 alone or in the presence of 10 µM BSA, 10 µM LbHop or 10 µM LbHop^{TPR2AB} was measured to verify the specificity of the co-chaperone inhibitory effect.

with their binding grooves pointing to opposite directions; thus, the interaction with convex regions of TPR2A-TPR2B causes Hsp90 to adopt a conformation that prevents its ATPase activity [27,31]. The LbHop and LbHop^{TPR2AB} constructs harbor this linker region; thus, our inhibition results are in agreement with those from Sti1.

3.7. Hop/Sti1 structural conservation: importance for chaperone function

Molecular chaperones are able to interact with a multitude of client proteins. To bypass this promiscuous binding behavior,

chaperones typically have short-lived and low-affinity interactions, avoiding the interference with the client protein activity [55]. A further mechanism for regulating chaperone function lies in the fact that these proteins act through an orchestrated range of interactions with co-chaperones. These assistant proteins influence the chaperone ATPase activity and may guide Hsp90 to select client proteins; additionally, in some cases, co-chaperones present intrinsic chaperone activity and their own interaction network [55]. Although Hsp70 and Hsp90 from different organisms display high sequence, structural and functional conservation, the sequence similarity among co-chaperone orthologous seems more divergent [30,56,57]. A study noted that none of the 10 Hsp90 co-chaperones analyzed using the genomes of 19 divergent species was present in all species [58]. This finding should suggest that the function of some co-chaperones may be related to a specific group of client proteins or that they may be required for client protein activation in a species-dependent manner [58]. The difference in the co-chaperone repertoire in divergent organisms suggests that some aspects of the chaperone/co-chaperone relationship may be differentially modulated across the species, providing another source of flexibility to the chaperone machine [58].

One interesting example of this observation lies in the Hop/Sti1 co-chaperone. Despite the low identity shown for LbHop and its counterparts, its structural features, such as structure, modularity and flexibility, are fully conserved. This high conservation degree was also observed in our previous studies of Hsp90 co-chaperones, such as Aha1 and p23 of *Leishmania braziliensis* (namely LbAha1 and Lbp23) [43,52]. LbAha1 showed 23% and 30% sequence identity with the Aha1 from yeast and human, respectively. Similar to other orthologs, LbAha1 displays two domains connected by a flexible linker and a highly elongated shape [52]. Furthermore, its functional properties are also consistent with those found in the yeast and human counterparts, corroborating the maintenance of the modulation profile [52]. The Lbp23 studies demonstrated the putative presence of two p23 isoforms in organisms for which the life cycle encompass a transition from an insect to a mammalian host; this finding indicates a conservation in the *modus operandi* of this co-chaperone, despite the low sequence similarity among the variants [43]. Although quantitative differences were observed between the two isoforms of p23 belonging to *L. braziliensis*, such as differences in the substrate specificity, their structural features and interaction behaviors with Hsp90 are consistent with those observed in humans and yeast, further supporting the conservation of the activity [43]. Such observations reinforce that the low identity could provide specificity for client proteins in an inter- or intra-specific manner, whereas the structure and function are conserved.

Hop/Sti1, being present in 18 of the analyzed 19 species, is the most prevalent co-chaperone found in the Johnson & Brown study [58]. An *in silico* characterization of the protein demonstrated that Hop/Sti1 has a highly conserved structure [31] (Table 1). Comparison of the Hop/Sti1 sequence from 88 eukaryotic organisms indicated great diversity in the domains, with the DP1 domain (with the linker region connecting DP1 and TPR2A) and the TPR2B domain as the least and the most conserved regions, respectively. Models for the interaction between the Hop/Sti1 protein and Hsp90 from human, yeast and *Plasmodium falciparum* indicated a different number of interactions in each protein pair [31]. This result reinforces the hypothesis that co-chaperones modulate the chaperone activity in different organisms and that the fine-tuning of settings should reside in the species-specific sequence divergence among orthologous proteins. Further supporting the importance of the sequence divergence, the phosphorylation of Sti1 and hHop occur at different sites such that the influence of regulatory phosphorylation is species specific [19].

Corroborating this view, Hsp70 belonging to prokaryotes display among 50–70% of sequence identity [59]. LbHsp90 showed an identity of about 63% with hHsp90α and yHsp90 [33]. In contrast, the Hop/Sti1 of these organisms shares an identity of approximately 35% (our work noted that orthologues Hop/Sti1 proteins share identities of approximately 30–40%, except for those belonging to closely related organisms, e.g., *L. braziliensis* and *L. major*). The studies performed with each protein pair demonstrated that they interact in the same manner and that the TPR2A-TPR2B-DP2 domain is both the main domain responsible for the interaction with Hsp90 and sufficient to inhibit the ATPase activity of Hsp90. Although the effects of the sequence differences between Hop/Sti1 proteins on their corresponding Hsp90 are not known, the divergences do not seem to influence the basic mechanism of interaction between them.

4. Concluding remarks

In this work, we provided a detailed presentation regarding the conservation, structure and function of the Hop/Sti1 co-chaperone of *L. braziliensis*. Our results indicated that LbHop and LbHop^{TPR2AB} behave as elongated monomers in solution; they are able to interact with LbHsp90 with the same affinity and can promote the inhibition of ATPase activity, as observed for Sti1 and hHop. Moreover, LbHop is a multidomain protein, a known characteristic of chaperones and co-chaperones [60], and its size enables the coupling of both the Hsp90 C- and M-domains as well as Hsp70. For LbHsp90, the interaction is accompanied by a restriction in the freedom of motion; we also observed this restriction in other co-chaperones interaction studies [43,52], and it may lead to the inhibition of LbHsp90 ATPase activity. Interestingly, these effects were dependent on both the TPR2A and TPR2B domains because the properties of the LbHop^{TPR2AB} construct were similar to those of the full-length protein.

The Hsp70 and Hsp90 chaperones are highly conserved within the three main phylogenetic branches, suggesting the importance of the mechanisms in which they are involved [57]. The mechanism of action of both chaperones is closely related to the interaction with co-chaperone proteins. Thus, the relative low sequence similarity found for the co-chaperones, in contrast to the high similarity presented by Hsp70 and Hsp90, is intriguing [30,57]. The convergent behavior of LbHop, compared with that of its orthologous proteins, could give the false idea that the relationship of the co-chaperone with chaperones is straightforward and unvarying in different organisms. Although this possibility could not be a rule of thumb, the structural features do not conform to the extent of sequence divergence of co-chaperones. Such observations provide the opportunity to explore the differences in the species-specific co-chaperone repertoire. Despite the overall structure and function conservation, differences in co-chaperone binding sites, including substrate-specific sites, might be explored to selectively disrupt the molecular chaperone system of protozoa.

Acknowledgments

CHIR, JCB and LRSB are CNPq Research Fellows and thank FAPESP and CNPq for financial support (#2011/23110-0, #2012/50161-8, #2014/07206-6 and #471415/2013-8). We also thank the LNLS/CNPEM-ABTLuS (Campinas, Brazil) staff for use of the SAXS beamline. We thank the LNBio/CNPEM-ABTLuS (Campinas, Brazil) for making the AUC device available.

References

[1] G.F. Späth, S. Drini, N. Rachidi, A touch of Zen: post-translational regulation of

the Leishmania stress response, Cell Microbiol. 17 (2015) 632–638.
[2] S. Brandau, A. Dresel, J. Clos, High constitutive levels of heat-shock proteins in human-pathogenic parasites of the genus Leishmania, Biochem. J. 310 (Pt. 1) (1995) 225–232.
[3] J. Clos, S. Krobitsch, Heat shock as a regular feature of the life cycle of *Leishmania* parasites, Amer. Zoll 39 (1999) 848–856.
[4] F.R. Opperdoes, G.H. Coombs, Metabolism of Leishmania: proven and predicted, Trends Parasitol. 23 (2007) 149–158.
[5] A. Hombach, J. Clos, No stress–Hsp90 and signal transduction in Leishmania, Parasitology 141 (2014) 1156–1166.
[6] M. Wiesgigl, J. Clos, Heat shock protein 90 homeostasis controls stage differentiation in Leishmania donovani, Mol. Biol. Cell 12 (2001) 3307–3316.
[7] R. Larreta, M. Soto, L. Quijada, C. Folgueira, D.R. Abanades, C. Alonso, J.M. Requena, The expression of HSP83 genes in Leishmania infantum is affected by temperature and by stage-differentiation and is regulated at the levels of mRNA stability and translation, BMC Mol. Biol. 5 (2004) 3.
[8] S. Krobitsch, J. Clos, A novel role for 100 kD heat shock proteins in the parasite Leishmania donovani, Cell Stress Chaperones 4 (1999) 191–198.
[9] T.V. Seraphim, C.H.I. Ramos, J.C. Borges, The interaction networks of Hsp70 and Hsp90 in the Plasmodium and Leishmania parasites, in: W. Houry (Ed.), The Molecular Chaperones Interaction Networks in Protein Folding and Degradation, Springer, New York, 2014, pp. 445–481.
[10] J.M. Eckl, K. Richter, Functions of the Hsp90 chaperone system: lifting client proteins to new heights, Int. J. Biochem. Mol. Biol. 4 (2013) 157–165.
[11] J. Li, J. Buchner, Structure, function and regulation of the hsp90 machinery, Biomed. J. 36 (2013) 106–117.
[12] H.H. Kampinga, E.A. Craig, The HSP70 chaperone machinery: J proteins as drivers of functional specificity, Nat. Rev. Mol. Cell Biol. 11 (2010) 579–592.
[13] M. Retzlaff, M. Stahl, H.C. Eberl, S. Lagleder, J.r. Beck, H. Kessler, J. Buchner, Hsp90 is regulated by a switch point in the C-terminal domain, EMBO Rep. (2009) 1147–1153.
[14] J.C. Borges, C.H. Ramos, Protein folding assisted by chaperones, Protein Pept. Lett. 12 (2005) 257–261.
[15] A. Walton-Diaz, S. Khan, D. Bourboulia, J.B. Trepel, L. Neckers, M. Mollapour, Contributions of co-chaperones and post-translational modifications towards Hsp90 drug sensitivity, Future Med. Chem. 5 (2013) 1059–1071.
[16] C. Scheufler, A. Brinker, G. Bourenkov, S. Pegoraro, L. Moroder, H. Bartunik, F.U. Hartl, I. Moarefi, Structure of TPR domain-peptide complexes: critical elements in the assembly of the Hsp70-Hsp90 multichaperone machine, Cell 101 (2000) 199–210.
[17] R.K. Allan, T. Ratajczak, Versatile TPR domains accommodate different modes of target protein recognition and function, Cell Stress Chaperones 16 (2011) 353–367.
[18] Y. Song, D.C. Masison, Independent regulation of Hsp70 and Hsp90 chaperones by Hsp70/Hsp90-organizing protein Sti1 (Hop1), J. Biol. Chem. 280 (2005) 34178–34185.
[19] A. Rohl, F. Tippel, E. Bender, A.B. Schmid, K. Richter, T. Madl, J. Buchner, Hop/Sti1 phosphorylation inhibits its co-chaperone function, EMBO Rep. 16 (2015) 240–249.
[20] C.T. Lee, C. Graf, F.J. Mayer, S.M. Richter, M.P. Mayer, Dynamics of the regulation of Hsp90 by the co-chaperone sti1, EMBO J. 31 (2012) 1518–1528.
[21] H. Wegele, M. Haslbeck, J. Reinstein, J. Buchner, Sti1 is a novel activator of the Ssa proteins, J. Biol. Chem. 278 (2003) 25970–25976.
[22] M. Roffé, F.H. Beraldo, R. Bester, M. Nunziante, C. Bach, G. Mancini, S. Gilch, I. Vorberg, B.A. Castilho, V.R. Martins, G.N. Hajj, Prion protein interaction with stress-inducible protein 1 enhances neuronal protein synthesis via mTOR, Proc. Natl. Acad. Sci. U. S. A. 107 (2010) 13147–13152.
[23] J.R. Webb, D. Kaufmann, A. Campos-Neto, S.G. Reed, Molecular cloning of a novel protein antigen of Leishmania major that elicits a potent immune response in experimental murine leishmaniasis, J. Immunol. 157 (1996) 5034–5041.
[24] Y. Goto, A. Bhatia, V.S. Raman, H. Liang, R. Mohamath, A.F. Picone, S.E. Vidal, T.S. Vedvick, R.F. Howard, S.G. Reed, KSAC, the first defined polyprotein vaccine candidate for visceral leishmaniasis, Clin. Vaccine Immunol. 18 (2011) 1118–1124.
[25] O.O. Odunuga, V.M. Longshaw, G.L. Blatch, Hop: more than an Hsp70/Hsp90 adaptor protein, Bioessays 26 (2004) 1058–1068.
[26] J. Demand, J. Lüders, J. Höhfeld, The carboxy-terminal domain of Hsc70 provides binding sites for a distinct set of chaperone cofactors, Mol. Cell Biol. 18 (1998) 2023–2028.
[27] A.B. Schmid, S. Lagleder, M.A. Gräwert, A. Röhl, F. Hagn, S.K. Wandinger, M.B. Cox, O. Demmer, K. Richter, M. Groll, H. Kessler, J. Buchner, The architecture of functional modules in the Hsp90 co-chaperone Sti1/Hop, EMBO J. 31 (2012) 1506–1517.
[28] C. Prodromou, G. Siligardi, R. O'Brien, D.N. Woolfson, L. Regan, B. Panaretou, J.E. Ladbury, P.W. Piper, L.H. Pearl, Regulation of Hsp90 ATPase activity by tetratricopeptide repeat (TPR)-domain co-chaperones, EMBO J. 18 (1999) 754–762.
[29] S. Alvira, J. Cuéllar, A. Röhl, S. Yamamoto, H. Itoh, C. Alfonso, G. Rivas, J. Buchner, J.M. Valpuesta, Structural characterization of the substrate transfer mechanism in Hsp70/Hsp90 folding machinery mediated by Hop, Nat. Commun. 5 (2014) 5484.
[30] J.L. Johnson, Evolution and function of diverse Hsp90 homologs and cochaperone proteins, Biochim. Biophys. Acta 1823 (2012) 607–613.
[31] R. Hatherley, C.L. Clitheroe, N. Faya, Ö. Tastan Bishop, Plasmodium falciparum Hop: detailed analysis on complex formation with Hsp70 and Hsp90, Biochem. Biophys. Res. Commun. 456 (2015) 440–445.
[32] I. Letunic, T. Doerks, P. Bork, SMART 7: recent updates to the protein domain annotation resource, Nucleic Acids Res. 40 (2012) D302–D305.
[33] K.P. Silva, T.V. Seraphim, J.C. Borges, Structural and functional studies of Leishmania braziliensis Hsp90, Biochim. Biophys. Acta 1834 (2013) 351–361.
[34] L. Whitmore, B.A. Wallace, DICHROWEB, an online server for protein secondary structure analyses from circular dichroism spectroscopic data, Nucleic Acids Res. 32 (2004) W668–W673.
[35] P.H. Brown, A. Balbo, P. Schuck, On the analysis of sedimentation velocity in the study of protein complexes, Eur. Biophys. J. 38 (2009) 1079–1099.
[36] J.C. Borges, C.H. Ramos, Analysis of molecular targets of Mycobacterium tuberculosis by analytical ultracentrifugation, Curr. Med. Chem. 18 (2011) 1276–1285.
[37] P.V. Konarev, V.V. Volkov, A.V. Sokolova, M.H.J. Koch, D.I. Svergun, PRIMUS: a Windows PC-based system for small-angle scattering data analysis, J. Appl. Crystallogr. 36 (2003) 1277–1282.
[38] D.I. Svergun, Determination of the regularization parameter in indirect-transform methods using perceptual criteria, J. Appl. Crystallogr. 25 (1992) 495–503.
[39] D.I. Svergun, Restoring low resolution structure of biological macromolecules from solution scattering using simulated annealing, Biophys. J. 76 (1999) 2879–2886.
[40] V.V. Volkov, D.I. Svergun, Uniqueness of ab initio shape determination in small-angle scattering, J. Appl. Crystallogr. 36 (2003) 860–864.
[41] A. Ortega, D. Amoros, J.G. de la Torre, Prediction of hydrodynamic and other solution properties of rigid proteins from atomic- and residue-level models, Biophy. J. 101 (2011) 892–898.
[42] E.F. Pettersen, T.D. Goddard, C.C. Huang, G.S. Couch, D.M. Greenblatt, E.C. Meng, T.E. Ferrin, UCSF chimera – A visualization system for exploratory research and analysis, J. Comput. Chem. 25 (2004) 1605–1612.
[43] F.A.H. Batista, G.S. Almeida, T.V. Seraphim, K.P. Silva, S.M.F. Murta, L.R.S. Barbosa, J.C. Borges, Identification of two p23 co-chaperone isoforms in Leishmania braziliensis exhibiting similar structures and Hsp90 interaction properties despite divergent stabilities, FEBS J. 282 (2015) 388–406.
[44] S.Y. Chen, D.F. Smith, Hop as an adaptor in the heat shock protein 70 (Hsp70) and Hsp90 chaperone machinery, J. Biol. Chem. 273 (1998) 35194–35200.
[45] B.D. Johnson, R.J. Schumacher, E.D. Ross, D.O. Toft, Hop modulates hsp70/hsp90 interactions in protein folding, J. Biol. Chem. 273 (1998) 3679–3686.
[46] L.M. Gava, D.C. Goncalves, J.C. Borges, C.H.I. Ramos, Stoichiometry and thermodynamics of the interaction between the C-terminus of human 90 kDa heat shock protein Hsp90 and the mitochondrial translocase of outer membrane Tom70, Arch. Biochem. Biophys. 513 (2011) 119–125.
[47] F. Yi, I. Doudevski, L. Regan, HOP is a monomer: investigation of the oligomeric state of the co-chaperone HOP, Protein Sci. 19 (2010) 19–25.
[48] D.C. Gonçalves, L.M. Gava, C.H. Ramos, Human Hsp70/Hsp90 organizing protein (Hop) D456G is a mixture of monomeric and dimeric species, Protein Pept. Lett. 17 (2010) 492–498.
[49] S.C. Onuoha, E.T. Coulstock, J.G. Grossmann, S.E. Jackson, Structural studies on the co-chaperone Hop and its complexes with Hsp90, J. Mol. Biol. 379 (2008) 732–744.
[50] A. Röhl, D. Wengler, T. Madl, S. Lagleder, F. Tippel, M. Herrmann, J. Hendrix, K. Richter, G. Hack, A.B. Schmid, H. Kessler, D.C. Lamb, J. Buchner, Hsp90 regulates the dynamics of its cochaperone Sti1 and the transfer of Hsp70 between modules, Nat. Commun. 6 (2015) 6655.
[51] F.A.H. Batista, L.M. Gava, G.M.S. Pinheiros, C.H.I. Ramos, J.C. Borges, From conformation to interaction: techniques to explore the Hsp70/Hsp90 network, Curr. Protein Pept. Sci. 16 (2015) 735–753.
[52] T.V. Seraphim, M.M. Alves, I.M. Silva, F.E. Gomes, K.P. Silva, S.M. Murta, L.R. Barbosa, J.C. Borges, Low resolution structural studies indicate that the activator of Hsp90 ATPase 1 (Aha1) of Leishmania braziliensis has an elongated shape which allows its interaction with both N- and M-domains of Hsp90, PLoS One 8 (2013) e66822.
[53] H. Wegele, S.K. Wandinger, A.B. Schmid, J. Reinstein, J. Buchner, Substrate transfer from the chaperone Hsp70 to Hsp90, J. Mol. Biol. 356 (2006) 802–811.
[54] D.R. Southworth, D.A. Agard, Client-loading conformation of the Hsp90 molecular chaperone revealed in the cryo-EM structure of the human Hsp90:Hop complex, Mol. Cell 42 (2011) 771–781.
[55] F.J. Echtenkamp, E. Zelin, E. Oxelmark, J.I. Woo, B.J. Andrews, M. Garabedian, B.C. Freeman, Global functional map of the p23 molecular chaperone reveals an extensive cellular network, Mol. Cell 43 (2011) 229–241.
[56] M.P. Mayer, B. Bukau, Hsp70 chaperones: cellular functions and molecular mechanism, Cell Mol. Life Sci. 62 (2005) 670–684.
[57] M.J. Figueras, P.C. Echeverria, S.O. Angel, Protozoan HSP90-heterocomplex: molecular interaction network and biological significance, Curr. Protein Pept. Sci. 15 (2014) 245–255.
[58] J.L. Johnson, C. Brown, Plasticity of the Hsp90 chaperone machine in divergent eukaryotic organisms, Cell Stress Chaperones 14 (2009) 83–94.
[59] F. Chiappori, M. Fumian, L. Milanesi, I. Merelli, DnaK as antibiotic target: hot spot residues analysis for differential inhibition of the bacterial protein in comparison with the human HSP70, PLoS One 10 (2015).
[60] J.C. Borges, T.V. Seraphim, P.R. Dores-Silva, L.R.S. Barbosa, A review of multidomain and flexible molecular chaperones studies by small-angle X-ray scattering, Biophys. Rev. 8 (2016) 1–14.